Available online at www.sciencedirect.com

SCIENCE DIRECT®

Journal of Geochemical Exploration 86 (2005) 86–103

JOURNAL OF GEOCHEMICAL EXPLORATION

www.elsevier.com/locate/jgeoexp

Influence of surface geology and mineral deposits on the spatial distributions of elemental concentrations in the stream sediments of Hokkaido, Japan

Atsuyuki Ohta *, Noboru Imai, Shigeru Terashima, Yoshiko Tachibana

Geological Survey of Japan, AIST, Central 7, 1-1-1 Higashi, Tsukuba, Ibaraki, 305-8567, Japan

Received 16 June 2004; accepted 4 April 2005

Abstract

An elucidation of the background levels of heavy metals, including certain toxic elements, is very essential to accomplish an important environmental assessment. A regional geochemical mapping in Hokkaido, Japan was undertaken by the Geological Survey of Japan, AIST as part of a nationwide geochemical mapping for this purpose. There were 692 stream sediments collected from the active channel (1 sample)/(100 km^2) in Hokkaido and the fine fraction sieved through a 180 μm screen was analyzed using the AAS, ICP-AES, and ICP-MS techniques. The regional geochemical maps for 51 elements were created as a 2000 m mesh map using the geographic information system software. Spatial distribution patterns of elemental concentrations in stream sediments, particularly Neogene–Quaternary volcanic and pyroclastic rocks, are primarily determined by surface geology. The correspondence of elemental concentrations in stream sediments to parent lithology is clearly indicated by ANOVA and a multiple comparison. Sediment samples supplied from mafic volcanic and felsic–mafic pyroclastic rocks are significantly rich in MgO, Al_2O_3, P_2O_5, CaO, Sc, TiO_2, V, MnO, Total (T)-Fe_2O_3, Co, Zn, Sr, and heavy rare earth elements (REEs) (Y and Eu–Lu), but significantly lacking in alkali elements, Be, Nb, light REEs (La–Nd), Ta, Tl, Th, and U. Accretionary complexes with sedimentary rocks derived from sediments are in stark contrast to volcanic and pyroclastic rocks. Accretionary complexes with mafic–ultramafic rock have significantly elevated Nb, Ta, and Th abundances in sediments besides MgO, Cr, Ni, Co, and Cu. This inexplicable result is caused by the mixed distributions of granite and ultramafic–mafic rocks.

The watersheds with mineral deposits relate to the high concentrations of certain elements such as Zn, As, and Hg. The geochemically anomalous pattern, which is a map of the regional anomalies, and a scatter diagram were applied to examine the contribution of mineral deposits to MnO, T-Fe_2O_3, Cr, Cu, Zn, As, Cd, Sb, Hg, Pb, and Bi concentrations. Consequently, they were grouped into four types: 1) Mineral deposits with no outliers resulting from mineralization (MnO, T-Fe_2O_3, and Cr), 2) sediments supplied from watersheds without metal deposits conceal high metal inputs from known mineral deposits (Cu), 3) deposits from a geochemically anomalous area that closely relates to the presence of mineral deposits (As, Sb, and Hg), and 4) deposits from the widely altered zone associated with the Kuroko as well as hydrothermal deposits corresponding to

* Corresponding author. Tel.: +81 298 61 3848; fax: +81 298 61 3566.
E-mail address: a.ohta@aist.go.jp (A. Ohta).

0375-6742/$ - see front matter
doi:10.1016/j.gexplo.2005.04.002

geochemically anomalous patterns (Zn, Cd, and Pb). This study provides an important regional geochemical database for a young island-arc setting and interpretational problems, such as complicated geology and active erosion, that are unique to Japan.

Keywords: Geochemical map; Geochemical anomaly; Stream sediment; Environmental assessment; Toxic element; Statistical analysis

1. Introduction

It is very essential to be familiar with the elemental abundance of, and the geochemical processes pertaining to, the earth's surface not only for mineral exploration but also for environmental assessment. European and North American countries have also prepared nationwide geochemical maps for the purpose of environmental assessment (Webb et al., 1978; Weaver et al., 1983; Fauth et al., 1985; Kautsky and Bølviken, 1986; Thalmann et al., 1988; Reimann et al., 1998; Gustavsson et al., 2001). In 1988, the International Geochemical Mapping Project (IGCP 259) was initiated under the auspices of UNESCO (Darnley et al., 1995). The IGCP 259 investigated the differences among the geochemical mapping of countries and standardized the method for creating a common database global geochemical baseline. The high-quality global multi-element geochemical database is expected to be useful for mineral resource exploration and environment protection.

On the other hand, in Japan, geochemical maps have only been prepared for limited areas: Akita Prefecture (Shiikawa et al., 1984), Northern Kanto region (Ito et al., 1991; Kamioka et al., 1991), and Aichi Prefecture (Tanaka et al., 1994; Yamamoto et al., 1998). Therefore, national geochemical mapping is required for the integration of sample materials, sampling methods, sampling density, grain size retained for analysis, analytical method, and a range of elements. Therefore, the Geological Survey of Japan, AIST (National Institute of Advanced Industrial Science and Technology) has initiated a nationwide geochemical mapping program at a scale of 1 : 2,000,000 in 1999 primarily for environmental assessment (Imai et al., 2001, 2004a,b). Nearly 3000 stream sediments were collected at a sampling density of 1 site per 80–120 km^2 throughout Japan. Imai et al. (2001), Mikoshiba and Imai (2003), and Ohta et al. (2004a,b, 2005) have discussed Tohoku, Hokuriku, Tokai, Kinki, and Chugoku regions in a nationwide geochemical map. In addition to national maps, the authors have also undertaken the geochemical mapping of the coast of the Sea of Japan (Imai et al., 1997; Ohta et al., 2004a) and an urban area that is possibly polluted by human activities (Ohta et al., 2002, 2003).

This paper describes the geochemical mapping for Hokkaido, the northern island of Japan. When interpreting spatial distributions of elemental concentrations, many controlling factors including surface geology, mineral deposits, and anthropogenic activity are taken into consideration. Hokkaido is richly endowed with nature and has relatively little anthropogenic pollution. Though the study area is extensively covered by Neogene–Quaternary volcanic rocks, its geology has distributions that are more complicated than those of Europe, the United States, and China. Hokkaido has abundant resources of heavy metals, such as Au, Ag, Hg, Mn, Zn, and Pb, which were mainly produced by Neogene volcanic activity. Some of those elements are toxic. An important element of an environmental assessment using a geochemical map is the understanding of the background levels of these toxic elemental concentrations. This study is intended to clarify the influence of surface geology and mineral deposits on elemental abundances of a young island-arc setting.

2. Methodology

The Hidaka Mountain is located in the central area, underlain by Mesozoic and Paleozoic rocks. Other geographical rises comprise Neogene–Quaternary volcanoes. The major rivers Ishikari and Tokachi form large coastal plains around Sapporo city and in the southeastern area, respectively. The sampling site was positioned upstream of the tributary from the junction of the main and subsidiary streams so as to avoid the accumulation of sediment that flows backward during a flood. The samples, weighing approximately 1–3 kg, were collected at the center of an active channel. A total of 692 stream sediments were collected from Hokkaido (Fig. 1) and the average sampling density was approx-

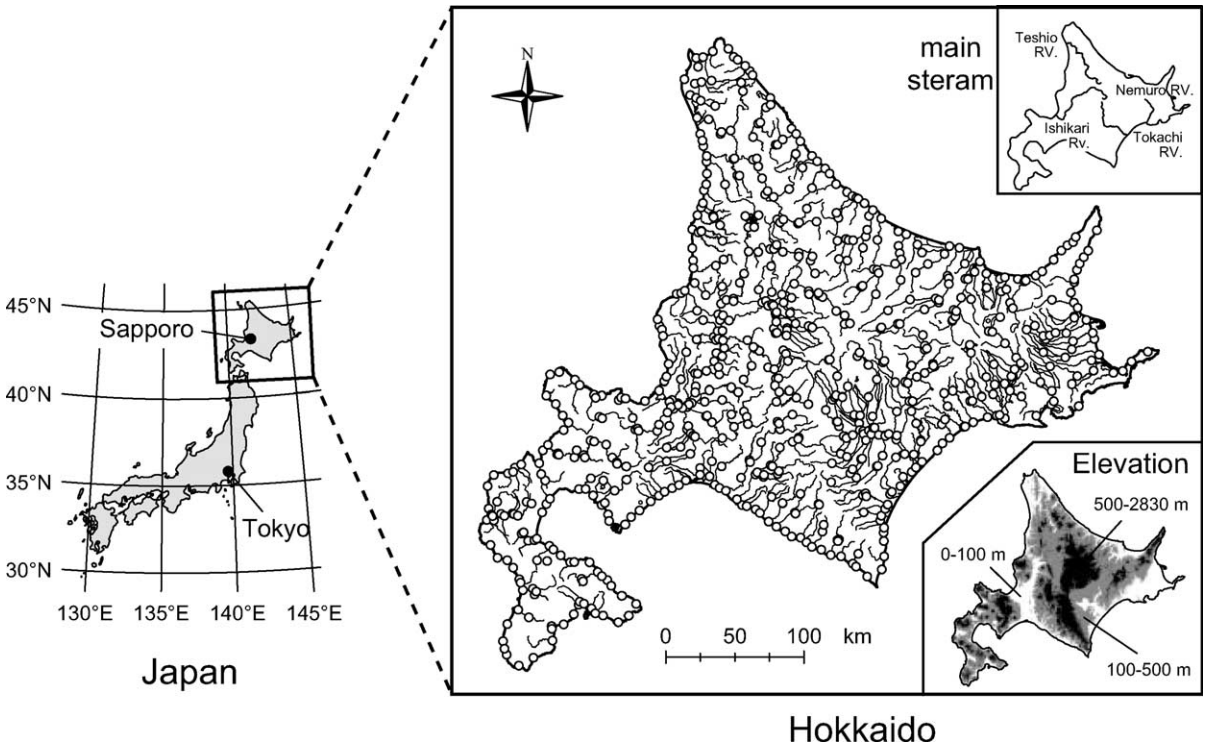

Fig. 1. Sampling locations of stream sediments (open circles) in Hokkaido. The solid line indicates the river.

imately 100 km^2. The samples collected were dried at room temperature and sieved using an 83-mesh (180 μm) screen; the fine fraction, however, was retained for analysis. Magnetite in the fine fraction was removed procedurally using a hand-held magnet.

Samples of stream sediment, weighing 0.2 g, were digested in HF, HNO_3, and $HClO_4$. This was based on the efficiency for decomposition of a large number of stream sediments (Imai, 1990). However, part of the heavy mineral fraction, particularly zircon, of the samples cannot be satisfactorily decomposed by this method. Nevertheless, incomplete decomposition of these minerals seriously affects a few elements such as Zr and Hf (Imai, 1987). The concentration of 49 elements was determined by the ICP-AES technique (Na_2O, MgO, Al_2O_3, P_2O_5, K_2O, CaO, TiO_2, MnO, Total Fe_2O_3 (T-Fe_2O_3), V, Sr, and Ba) and the ICP-MS technique (Li, Be, Sc, Cr, Co, Ni, Cu, Zn, Ga, Rb, Nb, Mo, Cd, Sn, Sb, Cs, rare earth elements (REE: Y and lanthanide), Ta, Tl, Pb, Bi, Th, and U). The As and Hg were separately analyzed by the AAS technique. A 0.2 g subsample was digested using HF, HNO_3, $HClO_4$, and $KMnO_4$ for As determination. In the case of the Hg analysis, an aliquot of a 1.0 g sample was treated with aqua regia. Table 1 summarizes the analytical results for stream sediments.

The accuracy of the analytical method was examined by repetitive measurements of NBS 1645 and GSD-1, which are stream sediments and Geochemical Reference samples of USA and China, respectively (Imai, 1987). The determined values were consistent with the reference or recommended values within 3% for 12 elements with the exception of K_2O and Pb. The precision of the determination was tested using certified refer-

Notes to Table 1:
Minimum (Min), maximum (Max), mean, median, standard deviation (S.D.), *p*-values of a Kolmogorov–Smirnov test for normality of the original (p) and log-transformed (p_log) data.
[a] $N=663$.
[b] $N=662$.

Table 1
Analytical results of stream sediments in Hokkaido region, Japan ($N=692$)

Element	Unit	Min	Max	Mean	Median	S.D.	p	p_log
Li	ppm	5.0	56.9	27.1	27.5	10.7	0.034	<0.001
Be	ppm	0.12	1.99	1.06	1.11	0.32	<0.001	<0.001
Na_2O	%	0.32	3.71	2.24	2.27	0.48	0.154	<0.001
MgO	%	0.89	14.1	3.40	3.01	1.63	<0.001	0.184
Al_2O_3	%	2.88	15.20	10.17	10.20	2.03	0.739	0.033
P_2O_5	%	0.03	0.73	0.13	0.12	0.06	<0.001	0.294
K_2O	%	0.09	2.61	1.45	1.52	0.47	0.002	<0.001
CaO	%	0.25	9.97	2.88	2.68	1.62	<0.001	<0.001
Sc	ppm	4.45	95.2	17.6	15.6	9.25	<0.001	0.555
TiO_2	%	0.17	4.94	0.94	0.79	0.53	<0.001	<0.001
V	ppm	38	561	159	142	69	<0.001	0.121
Cr	ppm	6	1334	85	58	103	<0.001	0.140
MnO	%	0.02	0.63	0.13	0.12	0.07	<0.001	0.200
T-Fe_2O_3	%	1.87	23.4	6.81	6.19	2.73	<0.001	0.037
Co	ppm	3.90	111	17.6	15.6	9.16	<0.001	0.626
Ni	ppm	1.87	2401	47.3	23.5	117	<0.001	<0.001
Cu	ppm	5.81	134	26.4	23.4	14.4	<0.001	0.935
Zn	ppm	37.1	939	104	91.9	57.1	<0.001	<0.001
Ga	ppm	5.74	23.4	15.1	15.1	2.23	0.006	<0.001
As[a]	ppm	0.5	870	12	6	38	<0.001	<0.001
Rb	ppm	2.70	125	51.3	51.8	23.5	0.075	<0.001
Sr	ppm	38.6	451	168	158	55.9	<0.001	0.492
Y	ppm	3.00	43.2	17.6	17.0	5.72	0.023	0.487
Nb	ppm	0.47	36.2	6.16	5.82	3.67	<0.001	<0.001
Mo	ppm	0.36	27.4	1.32	1.13	1.21	<0.001	0.535
Cd	ppm	0.02	5.19	0.15	0.10	0.28	<0.001	<0.001
Sn	ppm	0.51	21.3	1.64	1.48	1.22	<0.001	<0.001
Sb	ppm	0.09	12.1	0.72	0.47	0.94	<0.001	<0.001
Cs	ppm	0.20	20.6	3.75	3.46	2.22	<0.001	<0.001
Ba	ppm	65.1	2705	430	436	162	<0.001	<0.001
La	ppm	2.24	40.6	12.8	12.8	4.30	0.004	<0.001
Ce	ppm	5.87	81.2	24.0	23.4	8.09	<0.001	0.001
Pr	ppm	0.77	8.17	3.22	3.17	0.92	<0.001	0.003
Nd	ppm	3.18	33.3	13.4	13.1	3.46	<0.001	0.037
Sm	ppm	0.72	7.38	3.00	2.94	0.69	<0.001	0.204
Eu	ppm	0.20	1.91	0.82	0.81	0.20	0.136	0.491
Gd	ppm	0.69	7.58	2.96	2.88	0.73	0.008	0.299
Tb	ppm	0.13	1.35	0.54	0.52	0.14	0.080	0.629
Dy	ppm	0.69	6.94	2.87	2.81	0.83	0.073	0.719
Ho	ppm	0.14	1.37	0.58	0.56	0.18	0.011	0.595
Er	ppm	0.39	3.90	1.73	1.67	0.56	0.013	0.467
Tm	ppm	0.06	0.63	0.28	0.27	0.09	0.006	0.559
Yb	ppm	0.36	3.80	1.76	1.69	0.60	0.003	0.802
Lu	ppm	0.06	0.58	0.26	0.25	0.09	0.002	0.555
Ta	ppm	0.003	2.93	0.50	0.46	0.29	<0.001	<0.001
Hg[b]	ppb	10	10,530	132	60	563	<0.001	<0.001
Tl	ppm	0.01	1.83	0.38	0.38	0.18	<0.001	<0.001
Pb	ppm	4.07	194	17.6	14.7	14.7	<0.001	<0.001
Bi	ppm	0.02	13.10	0.25	0.18	0.56	<0.001	<0.001
Th	ppm	0.43	52.1	4.27	4.12	2.97	<0.001	<0.001
U	ppm	0.12	5.59	1.12	1.06	0.50	<0.001	<0.001

ence rock materials JB-3 (basaltic rock), and JSd-1 and JSd-3 (stream sediments). These internal reference materials were analyzed with every series of samples.

3. Geology and ore deposit

A 1 : 1,000,000 scale geological map of the Hokkaido area is shown in Fig. 2 (Geological Survey of Japan, 1992). Mesozoic and Paleozoic rocks are primarily distributed in central Hokkaido and partly in west and east Hokkaido. These are sedimentary and metamorphic rocks and accretionary complexes with ophiolite. Other areas are extensively covered by Neogene–Quaternary andesitic–dacitic lava, tuff, and pyroclastic rocks. On the other hand, small amounts of felsic volcanic rock and granite are sporadically distributed in western and central Hokkaido. Hokkaido is roughly divided into three regions — western, central, and eastern. This is useful in the discussion

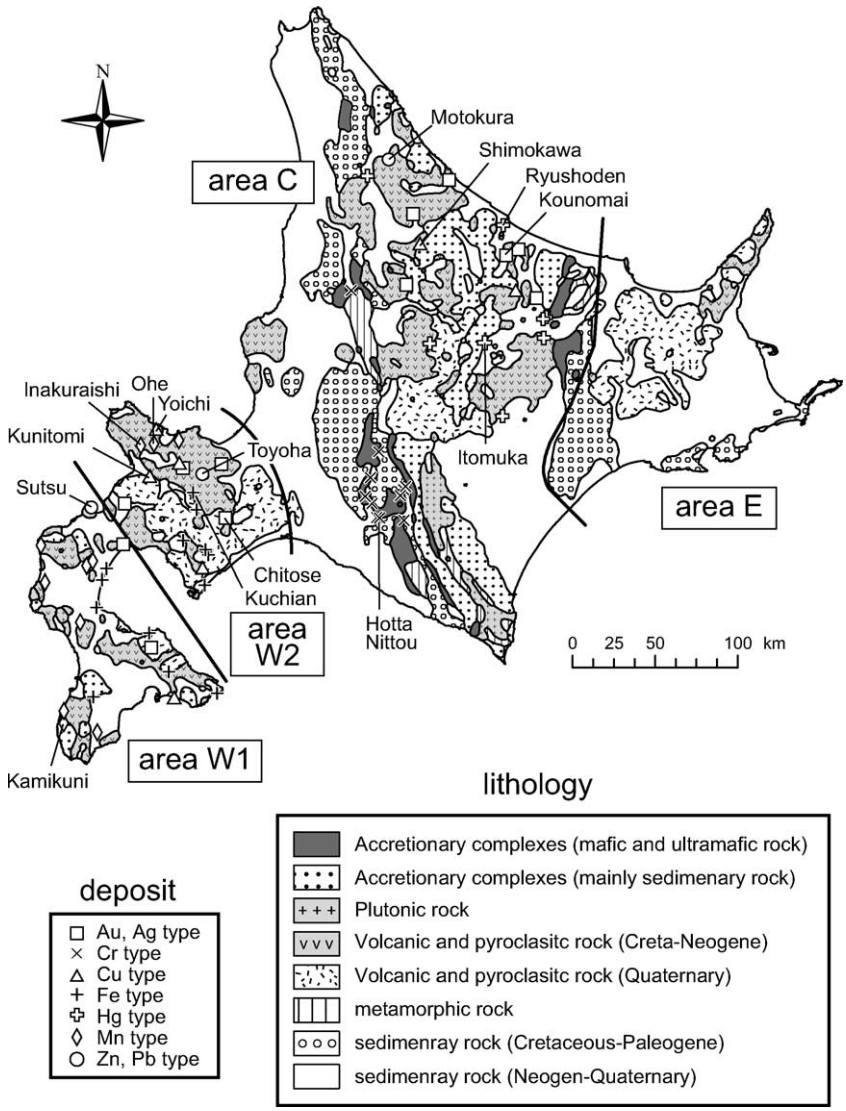

Fig. 2. Geological and mineral resource maps of the major deposits in Hokkaido prepared at a 1 : 1,000,000 scale (Kato et al., 1990; Geological Survey of Japan, 1992; Narita et al., 1996a,b). Hokkaido's geology is divided into four zones—areas W1, W2, C, and E—by solid lines.

related to the distributions of Tertiary geology (especially volcanic rocks) and natural resources (Kato et al., 1990). We used this division to conveniently refer to the western, central, and eastern parts as areas W, C, and E, respectively (Fig. 2). The western region of Hokkaido was expediently divided into two sub-areas (areas W1 and W2).

Fig. 2 also shows the distribution of major and economically mined deposits in Hokkaido (Kato et al., 1990; Narita et al., 1996a,b). Many mineral deposits are of the hydrothermal or disseminated type. They are closely related to the Neogene volcanic activity. Gold and silver deposits are found in the W2 area (Chitose mine), and to the northeast of area C (Kounomai mine); native gold, silver, and electrum being their main mineral ores. Mercury deposits are distributed primarily in the northeast of area C. The Itomuka mine is the largest mercury deposit in Japan and has a high ratio of native mercury to cinnabar. The W2 area has many zinc–lead (–copper) deposits. The Toyoha mine is the largest hydrothermal vein deposit (Zn, Pb, Ag, and In) in Japan. Other large-scale hydrothermal deposits are of the manganese type (Mn, Au, Ag, Zn, and Pb) and found in areas W1 and W2 (the Inakuraishi, Kamikuni, and Ohe mines). The Shimokawa mine, located to the northeast of area C, is the largest Cu deposit (Kieslager type) in Hokkaido. Although there are some hydrothermal and Kuroko-type copper mines in area W2 (Yoichi and Kunitomi mines), their economic yields are smaller than that of the Shimokawa mine. Other metallic ores are iron and chromium deposits. Iron deposits in Hokkaido are in the form of iron sands in area W1 and limonite (Kuchian mine) in areas W2 and C. Orthomagmatic chromium deposits are found in the vicinity of ultramafic rocks in area C (Nittou and Hotta mines). Sedimentary deposits such as alluvial gold and platinum also characterize Hokkaido. However, most elements analyzed here have barely any relation to these sedimentary type deposits.

4. Preparation for creating a geochemical map

Analyzed data were geographically visualized using the Geographic Information System (GIS) software. ArcGIS 8.3 (Environmental Systems Research Institute, Inc.) was used to prepare geochemical maps. The composition of stream sediment closely approximates the composite sample of the products of weathering and erosion of soil and rocks in the catchment area located upstream from the sampling site (Howarth and Thornton, 1983). Geochemical maps of the Hokkaido area that took watersheds into consideration were prepared as 2000 m grid maps according to Ohta et al. (2002, 2004a). The drainage basin system was generated from the digital elevation model provided by the Geographical Survey Institute, Japan. Several additional data points were newly generated within each river basin at intervals of 2000 m to conveniently depict the area by a set of points (Ohta et al., 2004a). An elemental concentration of each cell node (2000-m grid) was calculated from the surrounding 12 original and newly generated data points using the Inverse Distance Weight method (Watson and Philip, 1985). The scale for the geochemical map was classified using cumulative percentiles (5%, 10%, 25%, 50%, 75%, 90%, 95%, and 100%) (Reimann et al., 1998). However, since there are many samples within the detection limit (<10 ppb) of mercury, a different percentile (10%, 25%, 50%, 75%, 90%, 95%, and 100%) is used for the spatial distribution of the Hg content.

5. Results

5.1. Factor analysis of elemental concentrations in stream sediments

The geochemical subdivision of the Hokkaido district, Japan was made on the basis of factor analysis. This analysis assumes that the data distribution is either normal or Gaussian. There are two types of geochemical data distributions: normal and lognormal for many elements, particularly trace elements. The Kolmogorov–Smirnov test was conducted to estimate the normality of 51 elemental concentrations at the 0.01 significance level (Table 1). When the calculated probability exceeds 0.01, the elemental concentration is concluded to follow normality. Table 1 indicates that while only 10 elements for the original data follow normality, the log transformation procedure caused 24 elements to follow a normal distribution. The distributions of some elements are not normal even after log transformation. However, the log transformation reduces the skewness and kurtosis of their distributions in many cases (e.g., Ohta et al., 2002, 2004a). Conse-

quently, all elemental concentrations were transformed into common logarithms for factor analysis.

The author performed a principal factor analysis and used the Varimax procedure for factor rotation (Table 2). In order to reduce the number of variables, La and Yb were selected from REE. Four factors were selected, which explained 77% of the total variability,

Table 2
Factor loadings of a factor analysis carried out with 38 variables

Element	Comm.	Factor 1	Factor 2	Factor 3	Factor 4
Li	0.76	**−0.74**	−0.31	−0.03	−0.33
Be	0.87	**−0.88**	−0.23	−0.04	−0.21
Na_2O	0.57	−0.43	0.28	−0.44	0.35
MgO	0.80	0.23	**0.64**	−0.08	**−0.58**
Al_2O_3	0.45	−0.08	**0.65**	−0.10	−0.08
P_2O_5	0.22	0.13	0.34	0.27	0.10
K_2O	0.88	**−0.89**	−0.28	−0.11	−0.04
CaO	0.83	0.33	**0.83**	−0.07	0.19
Sc	0.90	0.41	**0.84**	0.07	−0.11
TiO_2	0.57	0.09	**0.71**	−0.09	−0.23
V	0.72	0.19	**0.77**	0.09	−0.31
Cr	0.86	−0.26	0.05	−0.20	**−0.86**
MnO	0.76	0.35	**0.76**	0.21	−0.10
T-Fe_2O_3	0.89	0.36	**0.78**	0.17	−0.35
Co	0.90	0.16	**0.62**	0.08	**−0.70**
Ni	0.82	−0.26	−0.09	−0.13	**−0.85**
Cu	0.35	−0.08	0.13	0.29	−0.49
Zn	0.59	0.18	0.45	**0.58**	−0.13
Ga	0.59	**−0.56**	**0.52**	0.04	0.04
As	0.46	−0.03	−0.05	**0.67**	0.00
Rb	0.90	**−0.84**	−0.42	−0.01	−0.11
Sr	0.53	−0.03	**0.60**	−0.26	0.33
Nb	0.68	**−0.60**	0.12	−0.01	**−0.55**
Mo	0.26	0.08	0.20	0.43	0.16
Cd	0.45	0.10	0.23	**0.61**	0.12
Sn	0.36	−0.44	0.01	0.37	−0.17
Sb	0.52	−0.15	−0.06	**0.70**	−0.03
Cs	0.63	**−0.67**	−0.25	0.34	0.01
Ba	0.52	**−0.67**	−0.12	0.13	0.19
La	0.70	**−0.80**	−0.06	−0.01	−0.22
Yb	0.60	0.17	**0.65**	0.15	0.36
Ta	0.60	**−0.54**	0.32	−0.04	−0.45
Hg	0.24	−0.21	−0.17	0.38	−0.15
Tl	0.80	**−0.75**	−0.27	0.40	0.06
Pb	0.52	−0.17	−0.03	**0.70**	0.07
Bi	0.55	−0.23	−0.05	**0.71**	−0.02
Th	0.58	**−0.74**	−0.13	0.05	−0.10
U	0.49	**−0.66**	−0.19	0.13	0.02
Eigen value		10.9	6.3	4.2	3.0
Variance (%)		35	20	13	9

Comm.: Communality.
Bold−faced type means that the factor loading is larger than 0.5 smaller than −0.5.

and the fifth factor was removed because of its low contribution rate (a mere 4%). Factor 1 (35%) is dominated by alkali elements Be, Ga, Nb, Ba, La, Ta, Tl, Th, and U (group 1). This reflects the contribution of granite and felsic volcanic rock. Factor 2 (20%) has high positive loadings for MgO, Al_2O_3, CaO, TiO_2, MnO, T-Fe_2O_3, Sc, V, Co, (Zn), Ga, Sr, and Yb. Factor 2 quantifies the contribution of mafic rocks (group 2). Factor 3 (13%) is dominated by Zn, As, Cd, Sb, Sn, Pb, and Bi and relates to mineral deposits such as Zn–Pb and Au–Ag type deposits (group 3). The association of MgO, Cr, Co, and Ni (and Cu) plays a role in factor 4 (group 4). Their concentrations are mainly controlled by ultramafic rock in accretionary complexes.

5.2. Spatial distribution patterns of elemental concentrations in stream sediments

The elements of the first association such as K_2O and Th have high concentrations in area C, which is primarily covered by sedimentary rocks and accretionary complexes (Fig. 3). These elemental concentrations in stream sediments are usually closely related to felsic volcanic rock, granite, and mudstone (melange) in accretionary complexes (Ohta et al., 2002, 2004a,b, 2005). These rock types are scarce in this region, but however, they influence the elemental abundances in sediments for this group. For example, the high enrichments of K_2O in the northeastern region of area C are explained by the distribution of sedimentaryrocks in accretionary complexes. Sporadically granitic outcrops in the eastern region of area W1 and southern part of area C strongly influence the REEs—Th and U (see Th in Fig. 3). Setting it into perspective, the spatial distribution patterns of this group adversely relate to the distributions of volcanic and pyroclastic rocks because the low concentration areas of K_2O and Th are covered by these rocks (Fig. 3).

The geochemical maps of the elements in group 2 are coherently related to the presence of volcanic and pyroclastic rocks. The high concentration area of Sc corresponds to the distribution of the Neogene–Quaternary volcanic and pyroclastic rocks (Fig. 3). As compared to these lithologies, mafic (basalt, basaltic rocks, amphibolite, and gabbro) and ultramafic rocks in accretionary complexes occurring in area C do not

strongly influence these elemental concentrations since their exposure is confined to small areas.

The Zn, As, Cd, Sb, Hg, Pb, and Bi playing a role in Factor 3 relates to the metallic mineral deposits in their distribution patterns. The high concentration area for these elements is located in the western and northeastern regions of Hokkaido (see Zn, As, and Hg in Fig. 3). The western region of Hokkaido has many Mn, Cu, Zn, Au, Ag, and Pb-type mineral deposits (Fig. 2). These mineral deposits result in high concentrations of Zn, As, Cd, Sb, Pb, and Bi in the western region of Hokkaido. The Au, Ag, and Hg deposits in the central and northeastern regions of Hokkaido are closely related to the spatial distribution pattern of the high concentration of As and Hg (Fig. 3). The geochemical maps for this association (with the exception of Zn) are not on the whole related to the distribution of surface geology. The high Zn concentration area in the western region of Hokkaido can be explained by mineral deposits and those in other regions, such as the eastern region of Hokkaido, can be explained by volcanic and pyroclastic rocks, similar to Sc in Fig. 3.

The mafic and ultramafic rocks in accretionary complexes strongly contribute to the elements of group 4. For instance, Fig. 3 shows geochemical maps for Cr and Cu. The spatial distribution pattern of high Cr concentration is consistent with that of ultramafic rock with chromium deposits. However, stream sediments from volcanic and pyroclastic rocks have a relatively low Cr content. Although ultramafic rock is not as highly rich in Cu as it is in Cr and Ni, the geochemical map for Cu is analogous to that for Cr. Some Cu deposits found in areas C and W2 do not always correspond to its high concentration areas. Consequently, the distribution pattern of the Cu concentration is controlled by mafic rock in accretionary complexes since these two lithologies are associated with each other.

6. Discussion

6.1. Influence of surface geology in the river basin

6.1.1. Selection of representative surface geology in the river basin

One of our interests is to ascertain the parent lithology that has a significant effect on the elemental concentrations of stream sediments. Previous studies for regional geochemical mapping in Japan suggested that a rock-type covering over more than half of the drainage basin area controls the elemental abundances in stream sediments (Ohta et al., 2002, 2004a,b and 2005). A total of 692 samples were classified into several subgroups on the basis of dominant geology. Hokkaido's geology is dominated by sedimentary, mafic volcanic and felsic–mafic pyroclastic rocks, and accretionary complexes (Fig. 2). Ultramafic–mafic rocks in accretionary complexes strongly affects the MgO, Cr, Co, Ni, and Cu contents regardless of their small exposures (Fig. 3). Therefore, a watershed whose major lithology is assigned to accretionary complexes with ultramafic– mafic rock is classified differently. In the case wherein no specific rock type extensively covers a catchment basin, the basin is classified as "the others." Table 3 presents the median of data subsets divided by the parent lithology for elements of group 1, 2, and 4 — the median is a robust value and is not subjected much to the influence of outliers (Ohta et al., 2005).

6.1.2. The statistical test of the effect of surface geology on elemental abundances in stream sediments

A comparison among several means is made by an analysis of variance (ANOVA) and the multiple comparison procedure (Hochberg and Tamhane, 1987; Nagata and Yoshida, 1997; Zhang and Wang, 2001). ANOVA was applied to the data subsets in order to conduct a statistical examination of the influence of surface geology on elemental abundances in sediments. Most elemental concentrations were transformed into common logarithms in order to satisfy the normality of the data. The Li, Be, Na_2O, Al_2O_3, K_2O, Ga, Rb, and La concentrations were not transformed since the normality of their original data is much better than that observed after lognormal transformation (Ohta et al., 2004a, 2005). The null hypothesis adopted in this case is that the elemental concentrations are the same among six data subsets. Table 3 also indicates that the probabilities calculated by ANOVA were lower than 0.05 for all the 43 elements. This result suggests that there are significant differences among sediments derived from the six rock types.

The Bonferroni test, which is one of the multiple comparison procedures, was then applied to the data at the confidence level of 0.05 to examine which data set differs significantly (follow-up test). There are

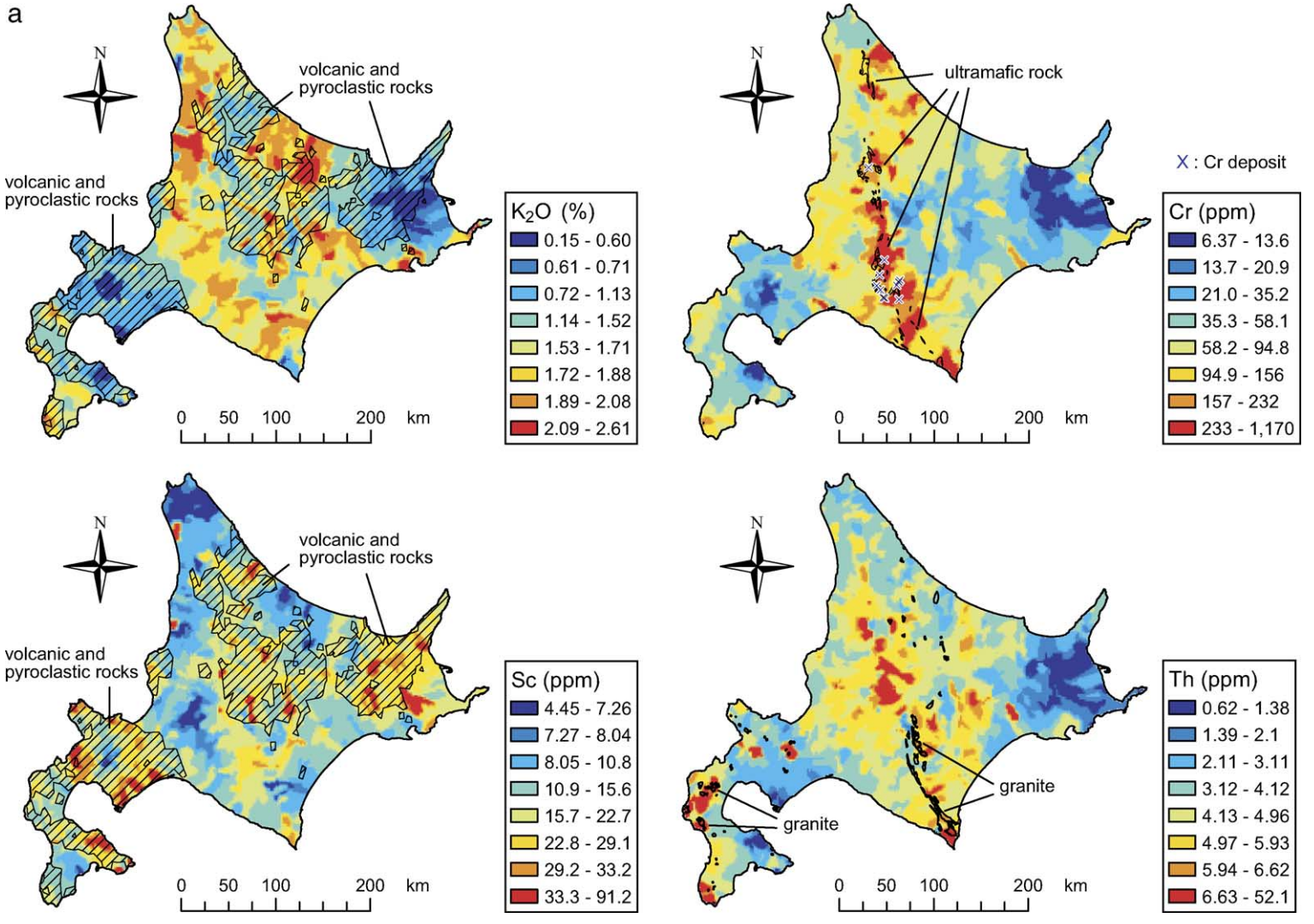

Fig. 3. a and b. The spatial distribution patterns of the K_2O, Sc, Cr, Cu, Zn, As, Hg, and Th concentrations. The scales for geochemical maps are classified by using the cumulative percentile (5%, 10%, 25%, 50%, 75%, 90%, 95%, and 100%). A different percentile (10%, 25%, 50%, 75%, 90%, 95%, and 100%) was used for Hg.

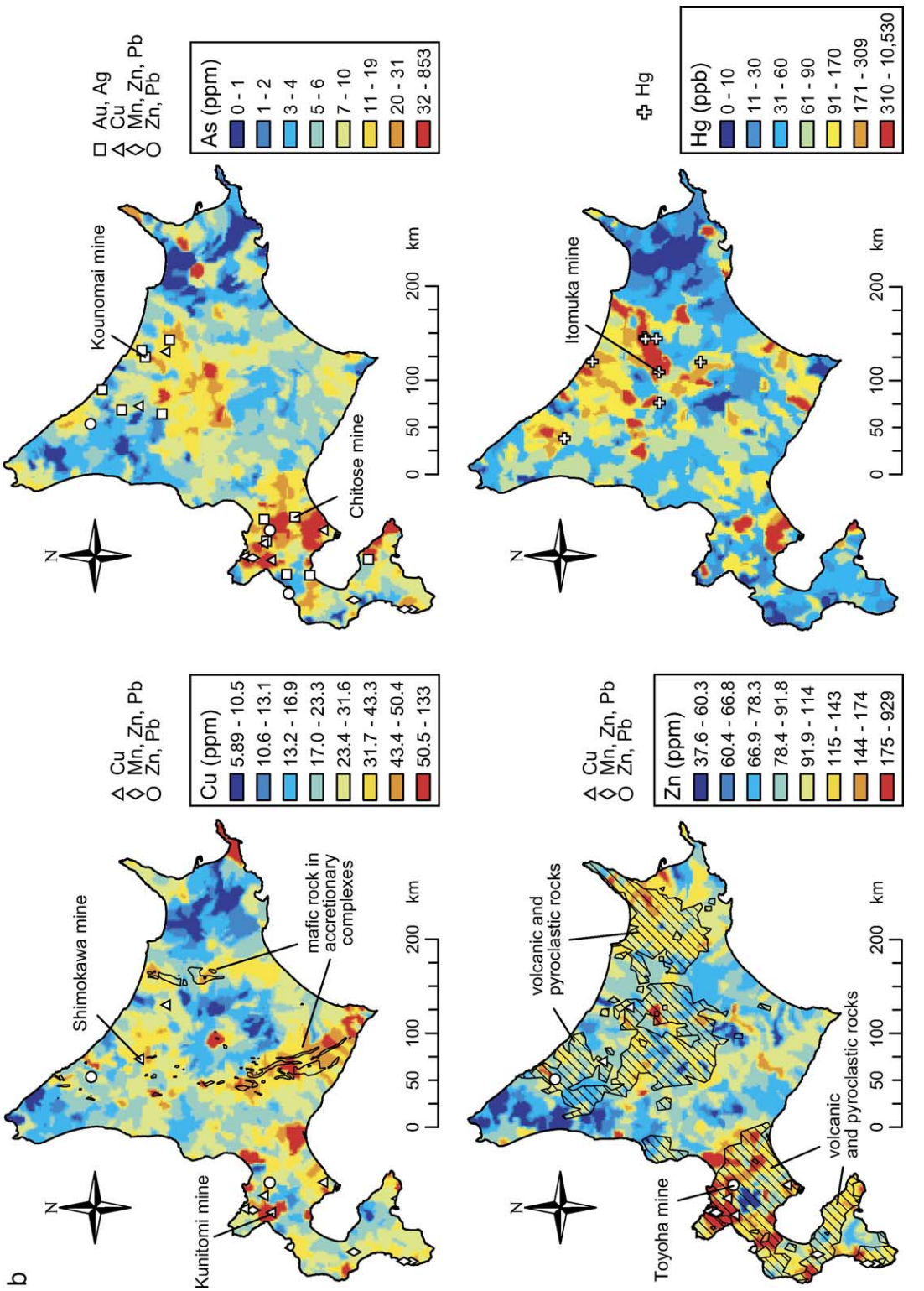

Fig. 3 (*continued*).

Table 3
Median of elemental concentrations of stream sediments for each parent lithology and significance probabilities (p) of one-way ANOVA

Parent lithology[a]		Sed	Acc_sed	Acc_um	Mv	Py	Oth	p
n		289	44	80	59	115	105	
Li	ppm	29	41	34	18	16	28	**<0.01**
Be	ppm	1.2	1.3	1.2	0.9	0.6	1.1	**<0.01**
Na_2O	%	2.4	2.3	2.2	2.1	2.6	2.2	**<0.01**
MgO	%	2.5	2.9	4.3	4.0	2.6	3.3	**<0.01**
Al_2O_3	%	9.0	10.6	11.0	11.8	10.4	10.5	**<0.01**
P_2O_5	%	0.11	0.11	0.11	0.13	0.14	0.13	**<0.01**
K_2O	%	1.6	1.9	1.7	1.1	1.0	1.4	**<0.01**
CaO	%	2.1	1.5	2.1	4.1	3.9	2.8	**<0.01**
Sc	ppm	12	12	15	23	20	17	**<0.01**
TiO_2	%	0.7	0.7	0.8	1.0	0.9	0.8	**<0.01**
V	ppm	122	136	141	205	150	151	**<0.01**
Cr	ppm	57	77	139	48	24	52	**<0.01**
MnO	%	0.09	0.10	0.11	0.16	0.15	0.14	**<0.01**
T-Fe_2O_3	%	5.3	5.4	6.2	8.0	6.5	6.5	**<0.01**
Co	ppm	13	15	23	21	14	16	**<0.01**
Ni	ppm	24	32	99	17	8	20	**<0.01**
Cu	ppm	22	32	33	24	15	25	**<0.01**
Zn	ppm	86	90	86	106	101	100	**<0.01**
Ga	ppm	15	16	15	16	15	15	**<0.01**
Rb	ppm	59	73	56	33	30	43	**<0.01**
Sr	ppm	156	134	138	188	163	153	**<0.01**
Y	ppm	15	13	16	19	23	18	**<0.01**
Nb	ppm	5.9	6.5	7.1	4.7	3.7	5.8	**<0.01**
Cs	ppm	3.5	4.4	3.3	2.9	2.6	3.8	**<0.01**
Ba	ppm	459	471	416	392	347	420	**<0.01**
La	ppm	13	15	14	11	9	13	**<0.01**
Ce	ppm	24	28	25	21	18	23	**<0.01**
Pr	ppm	3.2	3.7	3.4	2.9	2.6	3.2	**<0.01**
Nd	ppm	13	15	14	12	12	13	**<0.01**
Sm	ppm	2.8	3.0	3.0	3.0	3.0	3.0	**0.03**
Eu	ppm	0.76	0.76	0.79	0.88	0.87	0.85	**<0.01**
Gd	ppm	2.7	2.8	2.9	3.0	3.3	3.0	**<0.01**
Tb	ppm	0.48	0.49	0.52	0.55	0.65	0.56	**<0.01**
Dy	ppm	2.5	2.4	2.7	3.1	3.6	3.0	**<0.01**
Ho	ppm	0.50	0.46	0.53	0.61	0.75	0.61	**<0.01**
Er	ppm	1.5	1.3	1.6	1.9	2.3	1.8	**<0.01**
Tm	ppm	0.24	0.21	0.25	0.30	0.38	0.29	**<0.01**
Yb	ppm	1.5	1.2	1.5	1.9	2.5	1.8	**<0.01**
Lu	ppm	0.22	0.17	0.23	0.30	0.38	0.27	**<0.01**
Ta	ppm	0.44	0.50	0.60	0.40	0.32	0.49	**<0.01**
Tl	ppm	0.39	0.40	0.38	0.33	0.25	0.38	**<0.01**
Th	ppm	4.2	4.3	4.6	3.5	2.9	4.2	**<0.01**
U	ppm	1.2	1.0	1.1	1.0	0.8	1.0	**<0.01**

A bold-faced type means that the null hypothesis is rejected for $p=0.05$.

[a] The Sed, Acc_sed, Acc_um, Mv, Py and Oth show sedimentary rock, two kinds of accretionary complexes (sedimentary and ultramafic–mafic rocks), mafic volcanic, and felsic–mafic pyroclastic rocks and the other, respectively.

${}_6C_2=15$ possible combinations for the six-levels geology factors and the result was tabulated in Table 4. Tables 3 and 4 give evidence to the fact that magnitude relation of the median among parent lithologies derived from sediments is a reflection of the result of factor analysis.

Mafic-volcanic- and pyroclastic-rock-dominated drainage basins have significantly different content

Table 4
Results of the Bonferroni multiple comparison procedure at the 0.05 confidence intervall

Group 1[a]	Group 2[a]	Mean $_{Group\ 1}$ > Mean $_{Group\ 2}$[b]	Mean $_{Group\ 1}$ < Mean $_{Group\ 2}$[b]
Sed	Acc_sed	CaO, Sr, Er–Lu	Al_2O_3, Li, Be, Cr, Ni, Cu, Ga
Sed	Acc_um	Sr, Ba	MgO, Al_2O_3, T-Fe_2O_3, Sc, V, Cr, Co, Ni, Cu, Ga, Nb, Ce, Ta
Sed	Mv	Na_2O,K_2O, Li, Be, Rb, Ba, La, Pr, U	MgO, Al_2O_3, CaO, TiO_2, MnO, T-Fe_2O_3, Sc, V, Co, Zn, Ga, Sr, Y, Eu-Lu
Sed	Py	K_2O, Li, Be, Cr, Ni, Cu, Rb, Nb, Cs, Ba, La–Nd, Ta, TI, Th, U	Al_2O_3, P_2O_5, CaO, MnO, T-Fe_2O_3, Sc, Y, Eu–Lu
Sed	Oth	Na_2O, K_2O, Rb, Ba, U	MgO, Al_2O_3, CaO, MnO, T-Fe_2O_3, Sc, V, Co, Cu, Zn, Y, Sm, Gd–Lu
Acc_sed	Acc_um	Li	MgO, CaO, Cr, Co, Ni, Er–Lu
Acc_sed	Mv	K_2O, Li, Be, Cr, Ni, Cu, Rb, Nb, Cs, La-Pr	MgO, Al_2O_3, CaO, TiO_2, MnO, T-Fe_2O_3, Sc, V, Co, Zn, Sr, Y, Eu, Tb–Lu
Acc_sed	Py	K_2O, Li, Be, Cr, Ni, Cu, Rb, Nb, Cs, Ba, La–Nd, Ta, TI, Th	CaO, MnO, Sc, Sr, Y, Eu–Lu
Acc_sed	Oth	K_2O, Li, Be, Cr, Ni, Cu, Rb	CaO, MnO, Sc, Zn, Y, Tb–Lu
Acc_um	Mv	K_2O, Li, Be, Cr, Ni, Cu, Rb, Nb, La-Nd, Ta, Th	Al_2O_3, CaO, TiO_2, MnO, T-Fe_2O_3, Sc, V, Zn, Sr, Y, Dy–Lu
Acc_um	Py	MgO, K_2O, Li, Be, Cr, Co, Ni, Cu, Rb, Nb, La-Nd, Ta, TI, Th, U	Na_2O, P_2O_5, CaO, MnO, Sc, Sr, Y, Tb–Lu
Acc_um	Oth	MgO, K_2O, Li, Be, Cr, Co, Ni, Cu, Rb, Nb, Ta	Zn, Yb, Lu
Mv	Py	MgO, Al_2O_3, TiO_2, T-Fe_2O_3, Be, V, Cr, Co, Ni, Cu, Sr, Nb, La, Ce, Ta, TI	Na_2O, Y, Ho–Lu
Mv	Oth	MgO, Al_2O_3, CaO, TiO_2, T-Fe_2O_3, Sc, V, Co, Sr	K_2O, Li, Be, Rb, Cs
Py	Oth	Na_2O, CaO, Y, Dy-Lu	K_2O, Li, Be, Cr, Co, Ni, Cu, Rb, Nb, Cs, La–Nd, Ta, TI, Th

[a] The brevity code is the same as Table 3.
[b] Mean $_{Group\ 1}$ and Mean $_{Group\ 2}$ indicate the means of elemental concentrations in stream sediments derived from rock types listed under Groups 1 and 2, respectively.

from basins that are dominated by the other rock types. Sediments derived from these rocks are significantly richer in elements of group 2, such as T-Fe_2O_3, Sc, and HREEs, and significantly lacking in elements of group 1, such as K_2O and Rb (Tables 3 and 4). Nevertheless, the comparison between these two rock types suggests that sediments derived from mafic volcanic rocks are significantly richer in mafic elements, such as MgO, TiO_2, and T-Fe_2O_3, and significantly lacking in Na_2O, Y, and HREE (Eu–Lu) than the elements occurring in pyroclastic rocks. Factor analysis combined the influence of these two rock types on elemental abundances in stream sediments as Factor 2, but the multiple comparison procedure clearly distinguishes the respective features.

On the other hand, accretionary complexes with sedimentary rock contributes to significantly higher elemental abundances for group 1 and the depletion in elements of group 2 in stream sediments as compared to the other five lithologies. The contribution of this rock type to elemental abundances in stream sediment is contrary to those of volcanic and pyroclastic rocks. Stream sediments supplied from sedimentary rock also significantly depleted in the second association, but have no systematic significant enrichment of any

Table 5
The threshold determined by Smirnov–Grubbs test for a significance level of 0.05

Element	Threshold	Number
MnO	0.387%	6
T-Fe_2O_3	15.6%	9
Cr	249 ppm	29
Cu	67.0 ppm	13
Zn	203 ppm	22
As	26 ppm	42
Cd	0.274 ppm	46
Sb	1.65 ppm	49
Hg	235 ppb	43
Pb	33.1 ppm	35
Bi	0.517	29

elements, except for U among other rock types (Table 4). In conclusion, a spatial distribution pattern of most elements is controlled by the presence of volcanic and pyroclastic rocks.

Tables 3 and 4 suggest that sediments obtained from accretionary complexes with mafic–ultramafic rocks are significantly rich in Nb, Ta, and Th in addition to the fourth association (MgO, Cr, Ni, Co, and Cu). These three elements have large negative loadings for Factor 1 (Table 2) and are influenced strongly by the presence of granite (see Th in Fig. 3). The selection of granitic rock that was a representative of the surface geology in the river basin was combined with ultramafic and mafic rocks in accretionary complexes since they were located in close proximity to each other. Consequently, the result of the multiple comparison test is inconsistent with the visual interpretation (Fig. 3) and the end result of factor analysis (Table 2).

6.2. Influence of mineral deposits on the spatial distribution patterns of elements

In this section, the contribution of mineral deposits to the spatial distribution patterns of elements of group 3, and MnO, T-Fe_2O_3, Cr, and Cu are closely examined. A very high concentration of an element, a geochemical anomaly, is expected to be detected in a watershed with mineral deposits. The threshold of each element was determined by employing the Smirnov–Grubbs test for the original data at the confidence level of 0.05 in order to find a geochemical anomaly according to Ohta et al. (2004a,b). Table 5 tabulates the threshold and the number of outliers. The geochemically anomalous area selected by the threshold values are shown in Fig. 4a, b, and c.

As described above, stream sediments derived from mafic volcanic rocks and mafic–ultramafic rocks in accretionary complexes are highly enriched in MnO, T-Fe_2O_3, Cr, Cu, and Zn. The problem is that most mineral deposits relate to the Neogene–Quaternary volcanic activity and the Cr deposit is associated with ultramafic rock. Consequently, the influence of surface geology should be considered for the examination of relationships between a geochemical anomaly and mineral deposits. Toward this end, the scatter diagram between the elements related to a mineral deposit and Sc or Ni concentrations (Fig. 5) is prepared in order to differentiate between the contribution of surface geology and the geochemical anomaly since mineral deposits found in Hokkaido influence neither Sc nor Ni abundances.

6.2.1. Geochemically anomalous areas for Cr, MnO, T-Fe_2O_3 and Cu

The Cr, MnO, T-Fe_2O_3, and Cu play a role in Factor 2 or 4, but may be influenced by metalliferous deposits. Manganese ore is mainly hydrothermal and often includes zinc and lead ores and is distributed across areas W1 and W2. Iron deposits in Hokkaido are in the form of iron sand and limonite. However, only the limonite deposit is indicated in Fig. 4a because the magnetite in the samples was removed by a magnet. At a glance, these metallic deposits do not correspond to the geochemically anomalous areas for MnO and T-Fe_2O_3 (Fig. 4a). Table 5 suggests that the MnO and T-Fe_2O_3 concentrations have a small number of outliers. Moreover, the scatter plots in Fig. 5 indicate that the MnO and T-Fe_2O_3 concentrations correlate well with that of Sc. Therefore, spatial distribution patterns for MnO and T-Fe_2O_3 do not have significant contributions from mineral deposits.

The Cr and Ni are highly enriched in ultramafic rock, but chromite rarely includes Ni. An outlier observed in the scatter diagram is expected to relate to Cr deposits. Nevertheless, in actuality, the Cr content in the stream sediment is coherently related to the Ni content and does not include an outlier (Fig. 5). Furthermore, the distribution of the Cr deposit does not completely correspond to the geochemically anomalous pattern. The heterogeneity of chromite in stream sediments and unsatisfactory decomposition of chromite by HF, HNO_3, and $HClO_4$ might affect its spatial distribution. The close relationship between Cr and Ni contents in Fig. 5 concludes that the spatial distribution pattern of the Cr content is controlled by ultramafic rock; however, this is not very useful to detect the chromite ore deposits.

The distribution pattern of the Cu concentration is controlled by mafic rock in accretionary complexes, akin to those of Cr and Ni. The weak relation between the Cu and Ni concentrations (Fig. 5) confirms this conjecture. Accordingly, the scatter chart of the Cu and Ni concentrations is not necessary for the study of the influence of the Cu deposit on the Cu geochemical map. Fig. 4a shows a small Cu anomalous area in the

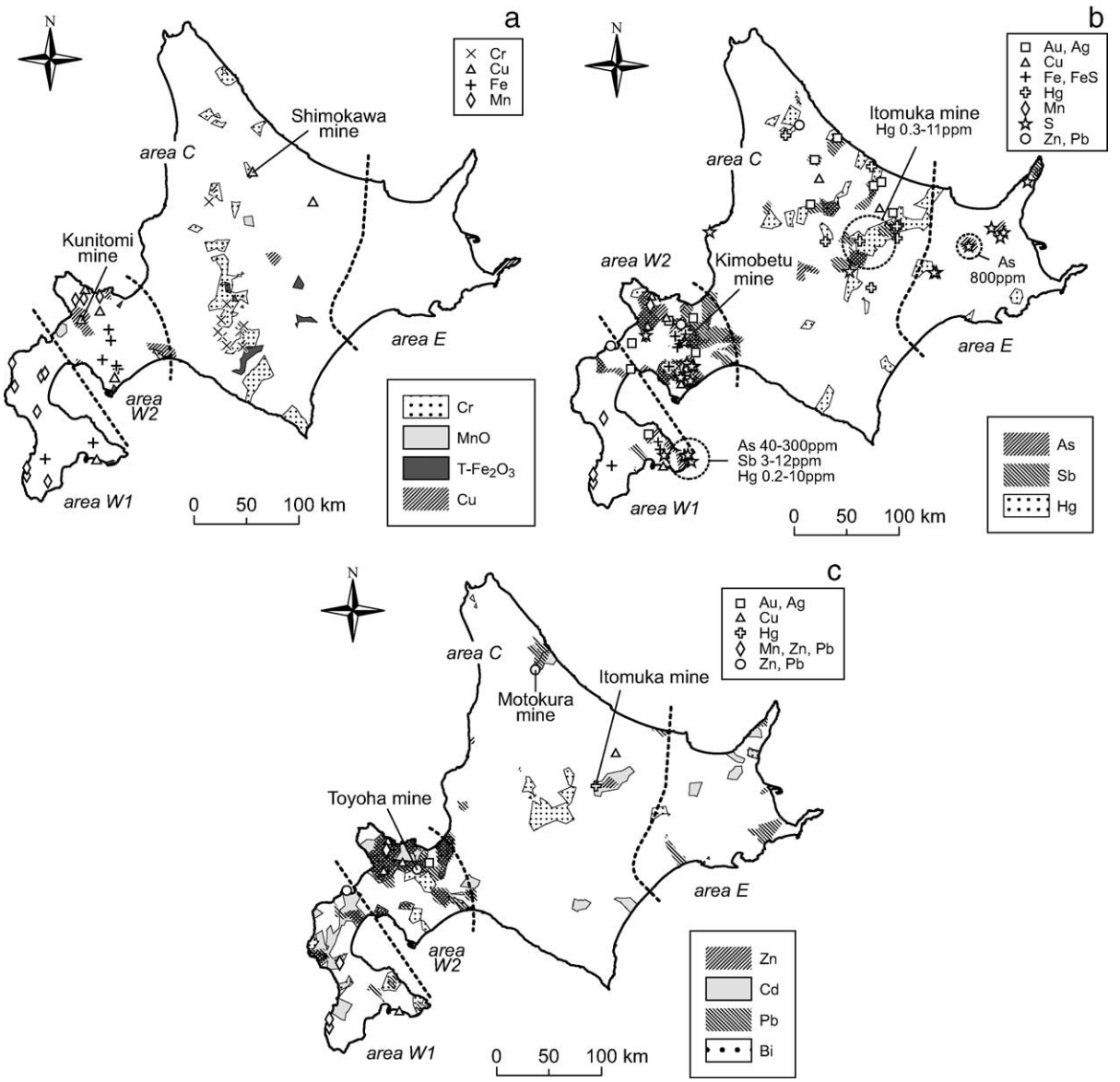

Fig. 4. a, b, and c. The geochemically anomalous patterns of MnO, T-Fe_2O_3, Cr, Cu Zn, As, Cd, Sb, Pb, Hg, and Bi concentrations selected by the threshold values exhibited in Table 5. The symbols of mineral deposits are the same as those in Fig. 3 except for sulfur and pyrite deposits (star symbol). Note that the Fe deposits except for sand iron are shown in a and b, and a part of the Mn and Cu deposits with Zn and Pb ores are indicated in b and c.

northern region of area W2 and they are caused by some Cu deposits such as the Kunitomi mine. However, other geochemical anomalies are unrelated to Cu mines. There is no anomalous feature even in the river basin with the Shimokawa mine, which is the largest Cu deposit in Hokkaido. Ohta et al. (2004a,b) reported that the influence of mineral deposits is restricted to a small area in the Hokuriku and Chugoku regions because active erosion resulting from high rainfall and steep mountains conceal its impact on elemental abundance. Consequently, it might be difficult to detect extreme geochemical anomalies related to mineral

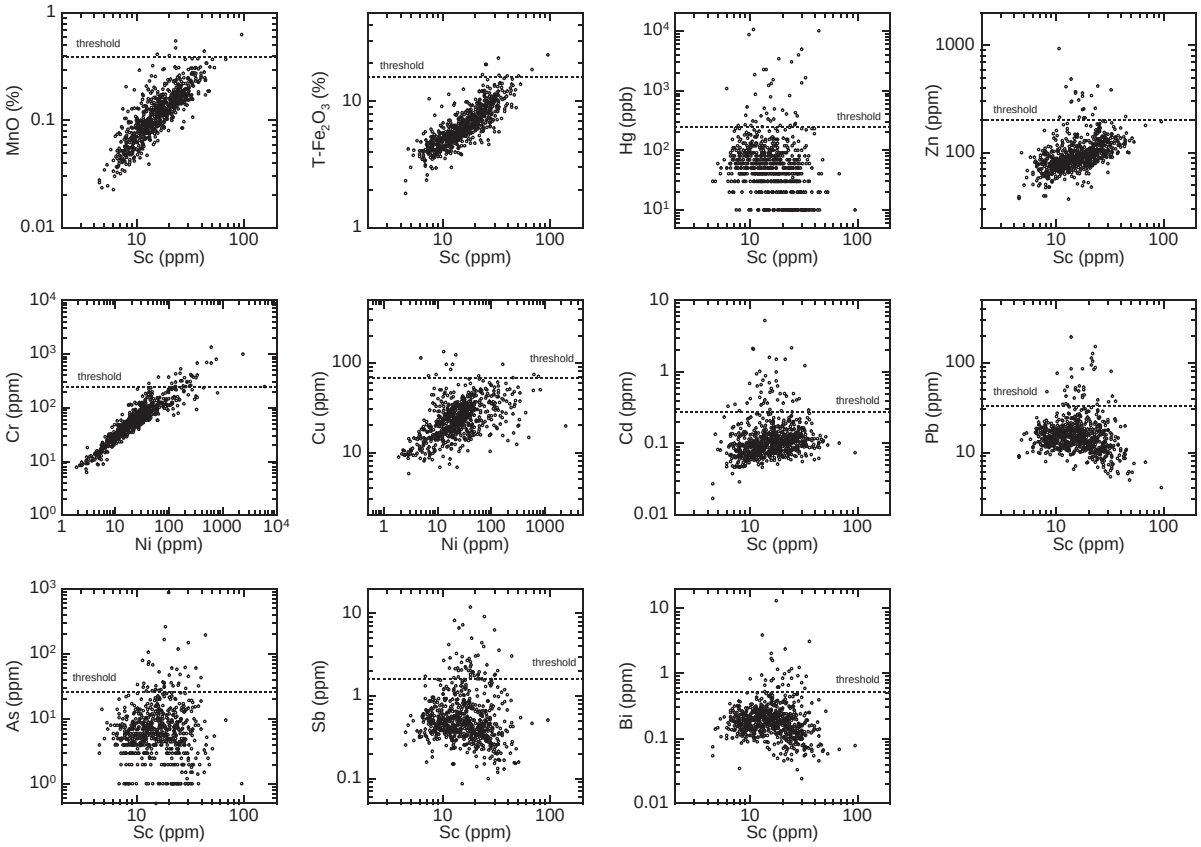

Fig. 5. Scatter diagrams of elemental concentrations in the stream sediments.

deposits unless the stream sediment sample is collected just downstream from the mineral deposit.

6.2.2. Geochemically anomalous areas for As, Sb, and Hg

The As, Sb, and Hg concentrations have either no relation or a weak relation to those of other elements (Fig. 5), which suggest that outliers should be related to any mineral deposits. Fig. 4b suggests that many anomalous patterns for As and Sb in area C and northern W2 correspond well to the Au–Ag and Cu–Zn–Pb deposits, respectively. Other high concentration areas do not relate to any deposits on the whole (Fig. 4b). The authors inferred that the Quaternary volcano strongly affects them despite the fact that undiscovered mineral deposits possibly have an influence on them. Quaternary volcanoes in Hokkaido are very active and sustain sulfur, pyrite, and limonite mining activity in many cases (Kato et al., 1990). For example, the Kimobetsu mine (limonite deposit) is renowned for its high concentration of As (Minato, 1998). The limonite deposit in area W2 and sulfur–pyrite deposits in areas W1, W2, and E are consistent with the geochemically anomalous patterns of As and Sb (Fig. 4b). Furthermore, stereoscopic observations revealed that these samples have many grains of sand rimmed with sulfur resulting from volcanic activity.

Fig. 4b shows that the distribution of Hg deposits in area C is consistent with the geochemically anomalous pattern. Extremely high concentrations of Hg downstream from the Itomuka mine and in its vicinity (330–10,530 ppb) suggested that the Hg minerals flow down the river from the mine in large quantities (Figs. 3 and 4b). Nevertheless, other anomalous regions in areas W1 and W2 are devoid of Hg deposits. In particular, the enclosed area in area W1 has extremely high Hg contents (2000–10,000 ppb) and is also highly enriched in As and Sb. These mercury anomalous

areas can be attributed to Quaternary volcanoes that lead to sulfur and pyrite deposits, such as As and Sb.

6.2.3. Geochemically anomalous areas for Zn, Cd, Pb, and Bi

The Zn and Cd concentrations correlate positively with the Sc concentration; however, the Pb content has weak or no correlation to the Sc content (Fig. 5). The samples selected above the respective threshold values do not have positive correlation to the Sc concentration anymore (Fig. 5). Geochemically anomalous areas for Zn, Cd, and Pb have much in common and are related to mining activity (Fig. 4c). The geochemical anomaly in the northern region of area W2 has many Zn–Pb deposits or Mn and Cu deposits bearing Zn and Pb ores. It is remarkable that the high concentration areas in area W2 are widely distributed outside the field of the Toyoha mine, which is the largest metalliferous deposit in Hokkaido (Fig. 4c). The miscellaneous map that Watanabe (2000) provided to examine the relationship among the mineralization potentiality, the hydrothermal system, and the geology in area W2 overcomes this inconsistency. According to the map, the north-central region of area W2 is covered by many hydrothermal alteration zones that are related to Kuroko deposits bearing Cu, Zn, and Pb and hydrothermal vein, replacement, and disseminated deposits associated with the Cu, Zn, Pb, and Mn ores. Geochemically anomalous areas in this region are very consistent with the hydrothermal alteration zones.

The areas W1 and E also have some anomalous areas for Zn, Cd, and Pb. The small area in the northern region of area C exhibiting high concentrations of Cd and Pb relate to the Motokura mine (Cu, Zn, and Pb type). The geochemical anomaly for Zn and Cd in area C is detected around the Itomuka mine (Hg deposit). Mineralization at the Itomuka mine might affect the enrichment of Zn and Cd. On the other hand, the geochemically anomalous areas in W1 and E do not match with the distribution of the metalliferous deposits. They indicate the presence of an alteration zone resulting from Neogene–Quaternary volcanic activities, similar to area W2, on account of the small or poor economical metalliferous deposits in these areas (Kato et al., 1990; Narita et al., 1996a,b).

The geochemically anomalous pattern of Bi is similar to those of Zn, Cd, and Pb in areas W1 and W2 (Fig. 4c). The southeastern region of area W1 and the central region of area C are also rich in Bi; however, they differ from the geochemically anomalous patterns of Zn, Cd, and Pb. The former area corresponds to the distribution of limonite, pyrite, and sulfur deposits such as As and Sb. The latter area is underlain by Neogene–Quaternary Tokachi–Taisetsu volcanoes and indicate a mineralization zone related to these volcanic rocks. Geochemically anomalous areas of Bi have features of both Zn–Cd–Pb and As–Sb.

7. Conclusion

In order to conduct an environmental assessment, background levels of 51 elements including some toxic elements, such as As and Hg, were assessed using a geochemical map. Most of the elements in the sediments reflect the parent lithology covering the drainage basin. The Zn, As, Cd, Sb, Hg, Pb, and Bi concentrations in the stream sediments have some extreme outliers resulting from mining activity pertaining to Au–Ag, Cu–Zn–Pb, FeS, Hg, Mn–Zn–Pb, and S deposits or a hydrothermal alteration zone. These results were very consistent with previous reports. However, complicated geology and active erosion make the interpretation of spatial distribution patterns of elements in stream sediments difficult. For example, the impact of Cu deposits on a geochemical map for Cu is concealed by stream sediments supplied from watersheds without mineral occurrences. The regional geochemical mapping in Hokkaido, Japan revealed the problems involved in understanding the background levels of elemental concentrations in a young island-arc setting (subduction zone) by using a geochemical map both quantitatively and objectively.

Acknowledgments

The authors thanks to M. Mikoshiba (Geological Survey of Japan, AIST) for her useful suggestion which help to improve the manuscript and grateful to D. Cohen (University of New South Wales) and one anonymous reviewer for their thoughtful and careful review of the manuscript.

References

Darnley, A.G., Björklund, A., Bølviken, B., Gustavsson, N., Koval, P.V., Plant, J.A., Steenfelt, A., Tauchid, M., Xuejing, X., 1995. A global geochemical database for environmental and resource management. Science Report, vol. 19. UNESCO, Paris (with contributions by Garrett, R.G. and Hall, G.E.M., 122 pp.).

Fauth, H., Hindel, R., Siewers, U., Zinner, J., 1985. Geochemischer Atlas Bundesrepublik Deutschland. BGR, Hannover. 79 pp.

Geological Survey of Japan, 1992. Geological Map of Japan, 1:1,000,000, 3rd, ed.

Gustavsson, N., Bølviken, B., Smith, D.B., Severson, R.C., 2001. Geochemical landscapes of the conterminous United States—New map presentations for 22 elements. USGS Prof. Paper 1648. 38 pp.

Howarth, R.J., Thornton, I., 1983. Regional geochemical mapping and its application to environmental studies. In: Thornton, I. (Ed.), Applied Environmental Geochemistry. Academic Press, pp. 41–73.

Hochberg, Y., Tamhane, A.C., 1987. Multiple Comparison Procedures. John Wiley and Sons Inc. 480 pp.

Imai, N., 1987. Multielement analysis of stream sediment by ICP-AES. Bunseki Kagaku 36, T41–T45 (in Japanese, with English abstr.).

Imai, N., 1990. Multielement analysis of rocks with the use of geological certified reference material by ICP-MS. Anal. Sci. 6, 389–395.

Imai, N., Terashima, S., Katayama, H., Nakajima, T., Ikehara, K., Taniguchi, M., 1997. Geochemical behavior of heavy metals in coastal marine sediments from the eastern margin of the Japan sea. Bull. Geol. Surv. Japan 48, 511–529 (in Japanese, with English abstr.).

Imai, N., Terashima, S., Okai, T., Kanai, Y., Mikoshiba, M., Kamioka, H., Togashi, S., Matsuhisa, Y., Taniguchi, M., Yokota, S., 2001. The geochemical map of domestic and foreign countries and new geochemical map project covering whole country in Japan. Chishitsu News 558, 9–17 (in Japanese).

Imai, N., Terashima, S., Ohta, A., Mikoshiba, M.U., Okai, T., Tachibana, Y., Togashi, S., Matsuhisa, Y., Kanai, Y., Kamioka, H., Taniguchi, M., 2004a. Geochemical map of Japan. Geological Survey of Japan, AIST. 209 pp. (in Japanese, with English abstr.).

Imai, N., Terashima, S., Ohta, A., Mikoshiba, M.U., Okai, T., Tachibana, Y., Togashi, S., Matsuhisa, Y., Kanai, Y., Kamioka, H., Taniguchi, M., 2004b. Database of elemental distribution (geochemical map) in Japan. Available at http://www.aist.go.jp/RIODB/geochemmap/.

>Ito, S., Kamioka, H., Tanaka, T., Togashi, S., Imai, N., Kanai, Y., Terashima, S., Uto, K., Okai, T., Ujiie, M., Shibata, K., Kamitani, M., Sato, K., Sakamoto, T., Ando, A., 1991. Geochemical Atlas of Japan—Northern Kanto Area. Geological Survey of Japan. 35 pp.

Kamioka, H., Tanaka, T., Itoh, S., Imai, N., 1991. Geochemical map of northeastern Kanto District, Japan. Chikyukagaku (Geochemistry) 25, 81–99 (in Japanese with English abstract).

Kato, M., Katsui, Y., Kitagawa, Y., Matsui, M., 1990. Regional Geology of Japan Part 1 (HOKKAIDO). Kyoritsu Shuppan Co. 354 pp. (in Japanese).

Kautsky, G., Bølviken, B., 1986. Geochemical Atlas of Northern Fennoscandia. Nordkalott Project. Geol. Surv. Sweden. 19 pp. with 144 maps.

Mikoshiba, M.U., Imai, N., 2003. Geochemical map of the Tohoku region, northern Honshu, Japan. Geochim. Cosmochim. Acta 67, A290 (abstr.)

Minato, H., 1998. Environmental Problems Regarding Arsenic Toxicity. Tokai University. 203 pp. (in Japanese).

Nagata, Y., Yoshida, M., 1997. Basic Multiple Comparison Procedures. Scientist Co., Ltd. 187 pp. (in Japanese).

Narita, E., Yajima, J., Ohta, E., Watanabe, Y., Hasaka, T., Hasaka, N., Hirano, H., Sudo, S., 1996a. Mineral Resources Map of Hokkaido (Eastern part), 1:500,000. Geological Survey of Japan.

Narita, E., Yajima, J., Ohta, E., Watanabe, Y., Hasaka, T., Hasaka, N., Hirano, H., Sudo, S., 1996b. Mineral Resources Map of Hokkaido (Western part), 1:500,000. Geological Survey of Japan.

Ohta, A., Imai, N., Okai, T., Endo, H., Kawanabe, S., Ishii, T., Taguchi, Y., Kamioka, H., 2002. The characteristics of chemical distribution patterns in and around Yamagata city—Geochemical map in the southern area of Yamagata Basin—. Chikyukagaku (Geochemistry) 36, 109–125 (in Japanese, with English abstr.).

Ohta, A., Imai, N., Okai, T., Endo, H., Ishii, T., Taguchi, Y., Kamioka, H., Mikoshiba (Ujiie), M., Terashima, S., 2003. Application of geochemical map around Sendai City to investigation of geochemical background and environmental assessment. Earth Science 57, 61–72 (in Japanese, with English abstr.).

Ohta, A., Imai, N., Terashima, S., Tachibana, Y., Ikehara, K., Nakajima, T., 2004a. Geochemical mapping in Hokuriku, Japan: influence of surface geology, mineral occurrences and mass movement from terrestrial to marine environments. Appl. Geochem. 19, 1453–1469.

Ohta, A., Imai, N., Terashima, S., Tachibana, Y., 2004b. Investigation of elemental behaviors in Chugoku region of Japan based on geochemical map utilizing stream sediments. Chikyukagaku (Geochemistry) 38, 203–222 (in Japanese, with English abstr.).

Ohta, A., Imai, N., Terashima, S., Tachibana, Y., 2005. Application of multi-element statistical analysis for regional geochemical mapping in Central Japan. Appl. Geochem. 20, 1017–1037.

Reimann, C., Äyräs, M., Chekushin, V., Bogatyrev, I., Boyd, R., Caritat, P. de., Dutter, R., Finne, T.E., Halleraker, J.H., Jæger, Ø., Kashulina, G., Lehto, O., Niskavaara, H., Pavlov, V., Räisänen, M.L., Strand, T., Volden, T., 1998. Environmental Geochemical Atlas of the Central Barents Region. Geological Survey of Norway, Trondheim, Norway. 745 pp.

Shiikawa, M., Kanayama, M., Takizawa, I., 1984. Geochemical map of Akita Prefecture. Dep. Geol. Akita University Publ. 29 pp. (in Japanese).

Tanaka, T., Kawabe, I., Hirahara, Y., Iwamori, H., Mimura, K., Sugisaki, R., Asahara, Y., Ito, T., Yarai, H., Yonezawa, C., Kanda, S., Shimizu, O., Hayashi, M., Miura, N., Mutoh, K., Ohta, A., Sugimura, K., Togami, K., Toriumi, T., Matsumura, Y., 1994. Geochemical survey of the Sanage-yama area in Aichi

Prefecture for environmental assessment. J. Earth Planet. Sci., Nagoya Univ. 41, 1–31.

Thalmann, F., Schermann, O., Schroll, E., Hausberger, G., 1988. Geochemical Atlas of the Republic of Austria. Geological Survey of Austria. 141 pp. with 35 maps.

Watanabe, Y., 2000. Miscellaneous Map Series 38, Magmatic—hydrothermal systems and related mineralization of late Cenozoic era in the Sapporo—Iwanai district, 1:200,000, Geological Survey of Japan.

Watson, D.F., Philip, G.M., 1985. A refinement of inverse distance weighted interpolation. Geo-Processing 2, 315–327.

Weaver, T.A., Broxton, D.E., Bolivar, S.L., Freeman, S.H.Geochemical Group, 1983. The geochemical atlas of Alaska. Earth and Space Sci. Div., Los Alamos Nat. Lab. (GJBX-32(83) US DOE. 57 pp.)

Webb, J.S., Thornton, I., Thompson, M., Howarth, R.J., Lowenstein, P.L., 1978. The Wolfson Geochemical Atlas of England and Wales. Oxford Univ. Press, Oxford. 74 pp.

Yamamoto, K., Tanaka, T., Kawabe, I., Iwamori, H., Hirahara, Y., Asahara, Y., Kim, K.H., Richardson, C., Ito, T., Dragusanu, C., Miura, N., Aoki, H., Ohta, A., Sakakibara, T., Tanimizu, M., Mizutani, Y., Miyanaga, N., Murayama, M., Senda, R., Takayanagi, Y., Inoue, Y., Kawasaki, K., Takagi, M., Nebu, S., Inayoshi, M., 1998. Geochemical map of the Ryoke granitic area in the northeastern part of Toyota City, Aichi Prefecture. J. Geol. Soc. Japan 104, 688–704 (in Japanese, with English abstr.).

Zhang, C., Wang, L., 2001. Multi-element geochemistry of sediments from the Pearl River system, China. Appl. Geochem. 16, 1251–1259.